Medical Physics
The International Journal of Medical Physics Research and Practice

Radiation dosimetry in digital breast tomosynthesis: Report of AAPM Tomosynthesis Subcommittee Task Group 223

Ioannis Sechopoulos, John M. Sabol, Johan Berglund, Wesley E. Bolch, Libby Brateman, Emmanuel Christodoulou, Michael Flynn, William Geiser, Mitchell Goodsitt, A. Kyle Jones, Joseph Y. Lo, Andrew D. A. Maidment, Kazuyoshi Nishino, Anita Nosratieh, Baorui Ren, W. Paul Segars, and Miriam Von Tiedemann

Citation: Medical Physics **41**, 091501 (2014); doi: 10.1118/1.4892600
View online: http://dx.doi.org/10.1118/1.4892600
View Table of Contents: http://scitation.aip.org/content/aapm/journal/medphys/41/9?ver=pdfcov
Published by the American Association of Physicists in Medicine

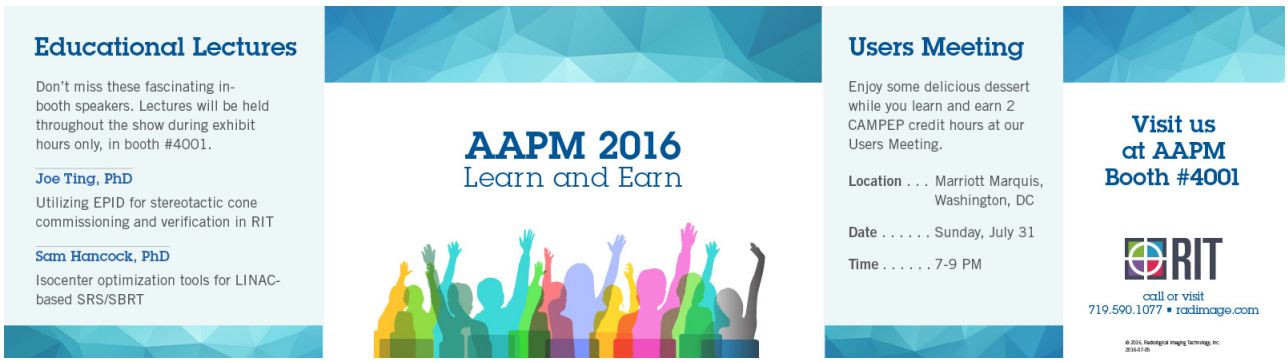

Radiation dosimetry in digital breast tomosynthesis: Report of AAPM Tomosynthesis Subcommittee Task Group 223

Ioannis Sechopoulos[a)]
Departments of Radiology and Imaging Sciences, Hematology and Medical Oncology and Winship Cancer Institute, Emory University, 1701 Uppergate Drive Northeast, Suite 5018, Atlanta, Georgia 30322

John M. Sabol
GE Healthcare, Global Diagnostic X-Ray, Mailstop W-701, 3000 North Grandview Boulevard, Waukesha, Wisconsin 53188

Johan Berglund
Research and Development, Philips Women's Healthcare, Solna, Sweden

Wesley E. Bolch
J. Crayton Pruitt Family Department of Biomedical Engineering, University of Florida, Gainesville, Florida 32611

Libby Brateman
University of Florida, Gainesville, Florida 32611

Emmanuel Christodoulou
Department of Radiology, University of Michigan, 1500 East Medical Center Drive, Ann Arbor, Michigan 48109

Michael Flynn
Department of Radiology, Henry Ford Health System, Radiology Research 2F, 1 Ford Place, Detroit, Michigan 48202

William Geiser
Department of Imaging Physics, The University of Texas MD Anderson Cancer Center, Houston, Texas 77030-4009

Mitchell Goodsitt
Department of Radiology, University of Michigan, 1500 East Medical Center Drive, Ann Arbor, Michigan 48109

A. Kyle Jones
Department of Imaging Physics, The University of Texas MD Anderson Cancer Center, Houston, Texas 77030

Joseph Y. Lo
Department of Radiology, Medical Physics Graduate Program, and Department of Biomedical Engineering, Carl E. Ravin Advanced Imaging Laboratories, Duke University, Durham, North Carolina 27705

Andrew D. A. Maidment
Department of Radiology, Perelman School of Medicine at the University of Pennsylvania, Philadelphia, Pennsylvania 19104-4206

Kazuyoshi Nishino
R & D X-ray Products Group, Shimadzu Corporation, Tokyo, Japan

Anita Nosratieh
Biomedical Engineering Graduate Group, Department of Radiology, University of California, Davis, California 95817

Baorui Ren
Hologic, Inc., 35 Crosby Drive, Bedford, Massachusetts 01730

W. Paul Segars
Department of Radiology, Medical Physics Graduate Program, and Department of Biomedical Engineering, Carl E. Ravin Advanced Imaging Laboratories, Duke University, Durham, North Carolina 27705

Miriam Von Tiedemann
PHILIPS Mammography Solutions, Solna, Sweden

(Received 18 February 2014; revised 27 June 2014; accepted for publication 23 July 2014; published 21 August 2014)

The radiation dose involved in any medical imaging modality that uses ionizing radiation needs to be well understood by the medical physics and clinical community. This is especially true of screening modalities. Digital breast tomosynthesis (DBT) has recently been introduced into the clinic and is

being used for screening for breast cancer in the general population. Therefore, it is important that the medical physics community have the required information to be able to understand, estimate, and communicate the radiation dose levels involved in breast tomosynthesis imaging. For this purpose, the American Association of Physicists in Medicine Task Group 223 on Dosimetry in Tomosynthesis Imaging has prepared this report that discusses dosimetry in breast imaging in general, and describes a methodology and provides the data necessary to estimate mean breast glandular dose from a tomosynthesis acquisition. In an effort to maximize familiarity with the procedures and data provided in this Report, the methodology to perform the dose estimation in DBT is based as much as possible on that used in mammography dose estimation. © *2014 American Association of Physicists in Medicine*. [http://dx.doi.org/10.1118/1.4892600]

Key words: breast tomosynthesis, dosimetry, Monte Carlo, mammography, breast cancer, mean glandular dose, conversion factor, relative glandular dose

1. INTRODUCTION

Radiation dosimetry in x-ray based breast imaging is concerned with the estimation of the dose to only the glandular tissues present in the imaged breast, since there is minimal risk of cancer development in the adipose tissues.[1] Therefore, the numerous studies reported on radiation dosimetry from mammography have used the *glandular dose* as the primary dose metric.[2–7] The dose estimations in these studies were performed using Monte Carlo simulations and the approximation of the imaged breast as composed of a homogeneous mixture of adipose and glandular tissue, with varying amounts of each tissue in the mixture. This homogeneity approximation is necessary due to two factors: (i) The computational complexity, especially in the early days, of simulating complex heterogeneous patterns of glandular/adipose tissue distribution and (ii) the natural variability of the glandular parenchyma in patients, making it impossible to simulate the infinite number of possible tissue distributions in human breasts. The homogeneity approximation, along with the use of a single dose value for the entire breast, gives rise to the term *mean glandular dose,* the metric actually estimated in mammography dosimetry studies. Although this metric does not represent an individual patient's dose and has the potential to result in an overestimation of actual patient glandular dose,[8] this metric does provide a method to compare the dosimetric consequences of different imaging technologies, acquisition techniques, and/or protocols. Finally, to relate the mean glandular dose estimate to the exposure level used for the study in question, the metric reported by mammography dosimetry studies is the *normalized mean glandular dose (D_gN)*, in which the mean glandular dose is normalized by a "reference" exposure or air kerma resulting from the imaging technique, at a pre-established point or area of reference. Therefore, the units of D_gN are dose per exposure (typically mGy/R) or dose per air kerma (typically mGy/mGy air kerma). Traditionally, the "reference" exposure has been defined as the exposure at the x-ray entrance surface of the breast under the compression paddle, denoted the entrance skin exposure (ESE). Due to this definition of the "reference" exposure, the exposure measured at one point in the x-ray beam (normally a few cm above the detector surface) is then adjusted by the inverse-square distance relationship to compute the ESE for breasts of varying thickness.

2. DOSIMETRY IN BREAST TOMOSYNTHESIS

Radiation dosimetry in breast tomosynthesis has, in general, been studied using the same methods as those used in mammography.[9–12] However, in tomosynthesis the possible variation in dosimetry due to the change in geometry during acquisition must be addressed. To determine the impact that the change in position of the x-ray tube (possibly accompanied by a rotation of the detector in some tomosynthesis systems[13]) has on dosimetry, including the change in distance between the tube and the entrance surface of the breast, the term *relative glandular dose* (RGD) has been introduced.[9,10] The RGD describes the change in the mean glandular dose between a zero-degree projection acquisition (equivalent to a mammography acquisition) and a projection acquisition at a non-zero angle using exactly the same imaging technique (target, filter, tube voltage, and tube current-exposure time product), therefore

$$\mathrm{RGD}(\alpha) = \frac{\mathrm{D_gN}(\alpha)}{\mathrm{D_gN}(0^\circ)}. \tag{1}$$

The RGD has been determined to be a function only of projection angle and breast size and thickness, being largely independent of x-ray spectrum and breast glandular fraction.[9] RGD can be used in combination with D_gN values for mammography (D_gN_{MAMMO}). When constant tube voltage and tube current-exposure time product are used for all projections, the following equation can be used for D_gN_{TOMO}:

$$\mathrm{D_gN_{TOMO}} = \mathrm{D_gN_{MAMMO}} \left(\frac{\sum_{\alpha=\alpha_{MIN}}^{\alpha_{MAX}} \mathrm{RGD}(\alpha)}{\mathrm{N}_\alpha} \right), \tag{2}$$

where D_gN_{TOMO} is the normalized glandular dose for a complete tomosynthesis acquisition, D_gN_{MAMMO} is the normalized glandular dose for a mammography acquisition, RGD(α) is the relative glandular dose at each projection angle α included in the tomosynthesis acquisition, and N_α is the total number of projections in the tomosynthesis acquisitions. For specific breast tomosynthesis systems with a fixed number of projections at fixed angular locations, Eq. (2) can be

simplified to the following:

$$D_gN_{TOMO} = D_gN_{MAMMO} \times \overline{RGD}, \quad (3)$$

where $\overline{RGD}$ is the mean RGD value for the complete breast tomosynthesis acquisition.

If an advanced acquisition protocol is used in which the tube current-exposure time product is varied among the projections, Eq. (2) needs to be modified, resulting in

$$D_gN_{TOMO} = D_gN_{MAMMO} \left(\frac{\sum_{\alpha=\alpha_{MIN}}^{\alpha_{MAX}} \frac{mAs_\alpha}{mAs_0} RGD(\alpha)}{N_\alpha} \right), \quad (4)$$

where mAs_α is the tube current-exposure time product used at projection angle α and mAs_0 is the tube current-exposure time product for the 0° projection.

In this report we provide RGD values for a generic system and the RGD and $\overline{RGD}$ values for five vendor-specific system designs. Given the low sensitivity of RGD to geometric variations, such as the vertical location of the center of rotation of the x-ray tube, we believe that the RGD values provided here for a generic system can be used for future commercial tomosynthesis systems. However, depending on the need for new values, the Tomosynthesis Subcommittee of the American Association of Physicists in Medicine might publish new system-specific RGD values in the future.

The D_gN_{MAMMO} data required for computation of D_gN_{TOMO} in combination with the RGD data provided in this report can be found in either of the previously published studies by Wu *et al.* for x-ray tubes with molybdenum and rhodium targets.[4,5] For other x-ray spectra or breast thicknesses not included in those publications, other sources of D_gN_{MAMMO} values are available, in both polyenergetic and monoenergetic form.[3,6,7,9–12,14,15] Additional D_gN_{MAMMO} values might be published in the future by the Mammography Subcommittee of the American Association of Physicists in Medicine.

To estimate the mean glandular dose for a breast tomosynthesis study using the information in this report and the mammography dosimetry data, the "reference" air kerma measurement should, in general, be performed as per the 1999 American College of Radiology (ACR) *Quality Control Manual*. However, due to the time-varying geometry during tomosynthesis acquisition (in particular, the oblique projection views), the following changes in measurement are needed: (i) one acquisition should be performed with the ACR phantom in its usual location and the technique selected by the automatic exposure control recorded; (ii) a second acquisition should be performed, using the previously recorded technique, without the phantom in place but with the dosimeter, in integrating mode, (ionization chamber or solid-state) placed at the midline of the detector in the chest wall direction (4 cm anterior to the chest wall edge) and at the typical measurement height above the detector, with the breast compression paddle placed at its maximum distance from the detector and a lead shield covering the detector. For full-field systems (i.e., excluding the Philips MicroDose and any other future slot-scan systems), if possible, the measurement should be performed in the acquisition mode that allows for the tomosynthesis target/filter combination to be used but with all exposures performed with the x-ray tube at the mammography (0°) position. If a static mode is not available, care should be taken to verify that the response of the dosimeter, especially if a solid-state dosimeter is used, is independent of the angle of incidence of the x-ray beam for the sweep angle studied. The smallest field of view that includes the entire sensitive volume of the dosimeter should be used, which might require an additional beam-limiting aperture in the raised paddle. In slot scan systems, the reduction of the field of view to minimize scatter contribution from the compression paddle is not needed due to the reduced x-ray beam area in this type of system.

The process to determine breast mean glandular dose from the data provided in this report is summarized in Fig. 1.

3. METHODS

3.A. Breast model

In this report we replicate the mammography model used by Wu *et al.*[4,5] Therefore, the breast was modeled in the cranio-caudal (CC) view as half an elliptical cylinder, with an 8 cm chest-wall to nipple distance and an 18 cm length along the chest-wall. The breast skin thickness was 4 mm, and the remaining breast tissue was composed of a homogeneous mixture of adipose and glandular tissue, with various weight fractions of 1%, 25%, 50%, 75%, and 100% glandular tissue. The chemical compositions of the three breast tissues were defined by Hammerstein *et al.*[1] The compressed breast thickness was varied from 2 to 9 cm, in 1 cm steps. Although the breast model used by Wu *et al.*[4,5] includes thicknesses only from 3 to 8 cm, 2 and 9 cm breast thicknesses are included in this report due to their prevalence in the clinic and the availability of mammography dose data for this thickness range from other sources, such as Boone.[7]

3.B. System model

All simulation details attempted to follow the Wu *et al.* model.[4,5] Specifically, the x-ray source was modeled as a point source that emits x rays only within the limits of the simulated detector. The x rays emitted were randomly sampled from a probability distribution function based on the spectral models provided by Boone *et al.*,[16] considering the corresponding added tube filtration and filtration due to a 2 mm thick polymethyl methacrylate breast compression paddle, a 1 mm thick Be window, a mirror [defined as a very thin layer of BoPET (Biaxially oriented polyethylene terephthalate) and aluminum] typically placed in the x-ray beam path for alignment of the light field, and the air between the x-ray source and the breast volume.

Figure 2 shows a diagram of a "standard" tomosynthesis system, including the x-ray source, breast compression paddle, breast support plate, compressed breast, and digital detector. In some systems, the detector rotates during acquisition, while in others it remains stationary. This diagram shows the simplified version of the geometry used for the simulations in this report, using the system parameters as listed in Tables I

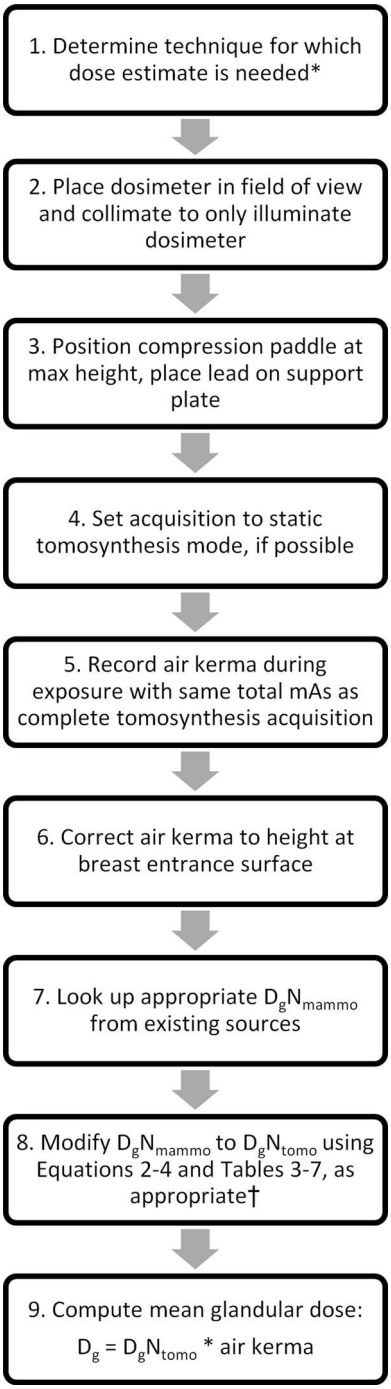

FIG. 1. Summary of process to determine breast mean glandular dose for a tomosynthesis acquisition from the data provided in this report. (*) Use a phantom such as the ACR accreditation phantom and record the technique determined by the AEC of the system or decide the technique of interest. (†) For the Philips slot scanning system, skip step 7 and use Eq. (6) and Table VIII.

and II. The geometry of the Philips MicroDose system is substantially different from that shown here, and it is discussed in Sec. 3.F.

3.C. Monte Carlo simulations

We used a previously validated[9] Monte Carlo simulation based on version 9.6 patch 02 of the Geant4 toolkit,[17,18] using

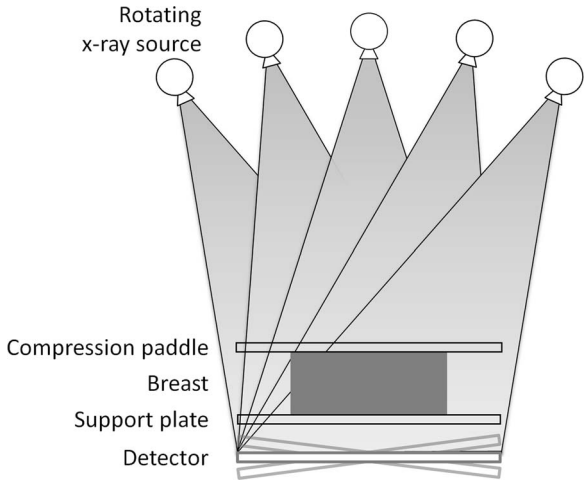

FIG. 2. Diagram of a typical breast tomosynthesis system. The x-ray source rotates around the compressed breast while the system acquires a limited number of projection images. Some system designs include detector rotation while in others the detector remains stationary.

the Livermore physics model for the electromagnetic interactions. During the simulation of each projection acquisition, 10^6 x rays were simulated from their emission by the x-ray source until their complete absorption or exit from the simulation limits. This number of x rays resulted in a statistical uncertainty lower than 0.6% for all simulations. The x rays could undergo photoelectric effect and Rayleigh and Compton scatter, according to the physics models used by the simulation. For every energy depositing event occurring within the adipose-glandular mixture breast tissue, the amount of energy deposited was recorded and weighted so as to obtain the energy deposited only in the glandular tissue portion of the mixture, using the equation:[6]

$$E_{G,DEP} = \frac{f_g \left(\frac{\mu_{en}}{\rho}\right)_g}{f_g \left(\frac{\mu_{en}}{\rho}\right)_g + (1 - f_g)\left(\frac{\mu_{en}}{\rho}\right)_a} E_{DEP}, \quad (5)$$

where $E_{G,DEP}$ is the energy deposited in the glandular tissue, E_{DEP} is the total energy deposited during the interaction in the breast tissue, f_g is the glandular fraction and $(\mu_{en}/\rho)_a$ and $(\mu_{en}/\rho)_g$ are the mass energy absorption coefficients of adipose and glandular tissue, respectively. To compute RGD(α), the total $E_{G,DEP}$ for the simulated projection at angle α was divided by the total $E_{G,DEP}$ resulting from the simulation of the zero degree projection.

Because it has been found that RGD does not vary substantially with x-ray spectrum and breast composition,[9] the RGD values reported here are the mean RGD values resulting from a range of these factors and are a function of breast thickness only. As mentioned, the range of breast compositions included is 1%–100% glandular density, while the range of x-ray spectra included in the simulations is specified in the tables describing the simulation parameters.

TABLE I. Generic tomosynthesis system specifications used to determine RGD values.

Imager size (cm)	24 × 30
Source to detector distance (cm)	66.0
Detector to x-ray tube center of rotation distance (cm)	0.0
Air gap (cm)	2.2
Number of projections	31
Angular range (deg)	±30
Detector rotation	No
Target/filter materials	W/50 μm Rh
Tube voltage (kVp)	23–39

3.D. Simulation parameters for generic breast tomosynthesis system model

Table I provides the specifications used to compute the RGD values for a generic theoretical breast tomosynthesis system. These parameters were chosen to reflect typical or average values found in commercial or prototype systems currently in existence. It should be noted that throughout this report, all projection angle information, including the angular range, is provided relative to the center of rotation, which is not necessarily located at the detector entrance surface.

3.E. Simulation parameters for specific breast tomosynthesis system models

Table II provides the specifications assumed to compute the RGD values for the specific breast tomosynthesis systems included in this report, based on the currently available public knowledge.[13]

3.F. Philips MicroDose tomosynthesis prototype system

The Philips MicroDose tomosynthesis prototype system is a scanning multislit full-field digital mammography system, which consists of a mammography x-ray tube, a multislit precollimator, and an image receptor, all mounted on a rigid scan arm (see Fig. 3). To acquire an image, the scan arm is rotated about a point below the detector so that the tube movement describes an arc above the object. Hence, each point in the object is viewed from a range of source-detector angles by different detector segments as the detector scans the object. This angular range (tomo angle) of 11° is determined most importantly by the width of the detector (50 mm or 4.6° from the tube focus point of view) and also by the angular range of the scan arm rotation (±15°). A large number of photon counting detector elements are read out continuously during a single scanning motion.

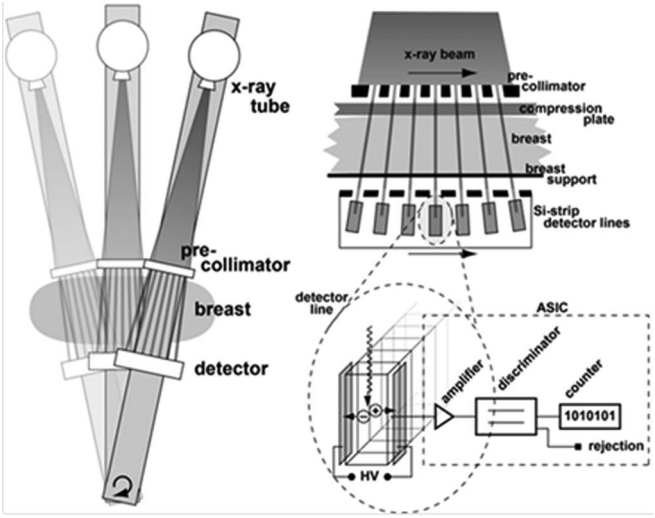

FIG. 3. Diagram of the Philips MicroDose tomosynthesis prototype system. (Left) An x-ray tube, a multislit precollimator, and a photon-counting detector are mounted on a scan arm, rotating about a point below the detector. (Right) The x-ray beam is collimated before entering the breast to match the 21 photon counting line detectors.

TABLE II. Breast tomosynthesis system specifications used in this report (Ref. 13). This information is believed accurate as of September 20, 2013. Modifications in the specifications of any of these systems may have an impact on the accuracy of the results provided in this report.

	GE SenoClaire	Hologic Selenia Dimensions	IMS Giotto TOMO	Philips MicroDose	Siemens MAMMOMAT Inspiration
Imager size (cm)	24 × 30	24 × 29	24 × 30	21 lines × 24 cm	24 × 30
Source to detector distance (cm)	66.0	70.0	68.0	66.0	65.5
Detector to x-ray tube center of rotation distance (cm)	4.0	0.0	2.0	−40.0	4.7
Air gap (cm)	2.2	2.5	2.2	0.4−2.4	1.7
Number of projections	9	15	13	(see text)	25
Angular range (deg)	±12.5	±7.5[a]	±20	11 (see text)	±23[b]
Detector rotation	No	Yes	No	Continuous slit scan	No
Target/filter material	Mo/Mo, Mo/Rh, and Rh/Rh	W/Al	W/Rh and W/Ag	W/Al	W/Rh
Filter material/thickness	Mo: 0.03 mm Rh: 0.025 mm	0.7 mm Al	Rh: 0.05 mm Ag: 0.05 mm	0.5 mm Al	0.05 mm Rh
Tube voltage (kVp)	Mo/Mo: 24–30 Mo/Rh: 26–32 Rh/Rh: 26–40	26–40	W/Rh: 23–35 W/Ag: 23–35	26–38	23–35

[a]The Hologic Selenia Dimensions allows for an alternative acquisition mode with an angular range of ±15°. This mode, however, is currently not approved for clinical use. Therefore the dosimetric data for this mode are provided in the Appendix.
[b]The x-ray tube rotation has a ±25° range, but the projections are acquired within the central ±23° of the total range of motion.

Given the differences in the acquisition geometry of the Philips system compared to the other tomosynthesis systems, it is necessary to use a different dosimetry method to estimate the glandular dose for a complete breast tomosynthesis acquisition. Specifically for this system, given a measurement of the "reference" air kerma (AK_{REF}), the glandular dose (D_g) can be estimated using the equation:

$$D_{g,TOMO} = D_g N_{TOMO} \times AK_{REF}, \quad (6)$$

where values for $D_g N_{TOMO}$ are provided in this report and the AK_{REF} should be measured as described in Sec. 2.

As opposed to the simulations for the other tomosynthesis systems, the Monte Carlo simulations for the Philips scanning system used a random projection angle for each simulated x-ray, within the angular range of the scan arm of the system. Upon selection of the source position for each x-ray, the possible emission direction of each was randomly selected to be within the angle subtended by the detector segments in their corresponding position. The interactions and processes that each x-ray underwent after emission were simulated in the same manner as for the other tomosynthesis systems, yielding the average breast glandular dose for each scan. A second simulation for each imaging condition was performed, with the breast volume replaced by a surface representing the entrance of the ion chamber, yielding the "reference" air kerma used for each simulation. The normalized glandular dose values were obtained by normalizing the simulated average breast glandular dose by the simulated "reference" air kerma. The simulations to estimate the former involved 10^6 x rays, while for the latter 50×10^6 x rays were simulated.

3.G. Validation of Monte Carlo simulations

The conditions simulated by Wu *et al.* were replicated as closely as possible and the results are compared to those included in that publication.[4] For this comparison, the compressed breast thickness ranged from 3 to 8 cm in steps of 1 cm, and the x-ray spectra were specified as those emitted by a molybdenum anode with an added 0.3 mm thick molybdenum filter, a compression paddle of approximately 2 mm and with tube voltages varying from 23 to 35 kVp in steps of 4 kVp. For each tube voltage target/filter combination, the thickness of the compression paddle hardening the x-ray spectrum was varied so that the first half-value layer of the spectrum incident upon the breast matched one of the first half-value layers of the corresponding spectra used by Wu *et al.*

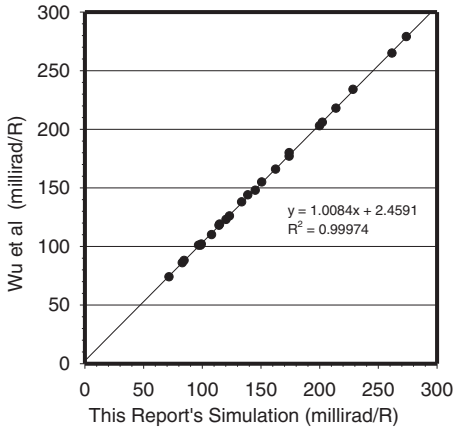

FIG. 4. Comparison of the normalized glandular dose for varying compressed breast thicknesses and x-ray spectra as estimated by the simulation used in this report and that published by Wu *et al.* (Ref. 4).

4. RESULTS

4.A. Validation of Monte Carlo simulations

Figure 4 compares the normalized mean glandular dose reported by Wu *et al.*[4] to that estimated by the Monte Carlo simulation used in this report. As can be seen, the results are very similar, with the slope of the linear fit having a value of 1.0084 (95% confidence interval: 1.0012–1.0157) and an offset value of 2.4591 millirad/R (95% CI: 1.3076–3.6107 millirad/R). Therefore, the simulation used in this report can be considered validated against previously published data.

4.B. Generic breast tomosynthesis system

Table III provides the resulting RGD values for the generic breast tomosynthesis system described in Table I. When calculating $D_g N_{TOMO}$ for a specific system, the appropriate RGD value(s) for the specific angles used by the system must be looked-up and/or interpolated from the table, and, together with the total number of projections and the value for the corresponding $D_g N_{MAMMO}$ from Wu *et al.*, be used as inputs to Eq. (1). If RGD values for angles larger than 30° are needed, these can be extrapolated from the data provided, as the RGD

TABLE III. RGD values for the generic tomosynthesis system.

Thickness	Angle (deg)															
(cm)	0	2	4	6	8	10	12	14	16	18	20	22	24	26	28	30
2	1.000	1.000	0.999	0.996	0.993	0.990	0.982	0.976	0.968	0.959	0.950	0.938	0.927	0.913	0.899	0.883
3	1.000	0.999	0.999	0.994	0.990	0.983	0.977	0.968	0.959	0.947	0.935	0.922	0.907	0.891	0.874	0.855
4	1.000	1.000	0.997	0.993	0.987	0.982	0.974	0.963	0.953	0.939	0.926	0.910	0.894	0.877	0.859	0.840
5	1.000	0.998	0.995	0.993	0.987	0.979	0.969	0.959	0.945	0.932	0.917	0.902	0.884	0.866	0.848	0.828
6	1.000	0.999	0.995	0.991	0.983	0.976	0.965	0.954	0.940	0.927	0.911	0.895	0.878	0.860	0.842	0.823
7	1.000	0.998	0.996	0.991	0.983	0.975	0.964	0.950	0.936	0.923	0.907	0.891	0.874	0.857	0.839	0.817
8	1.000	1.000	0.997	0.990	0.983	0.974	0.961	0.949	0.934	0.920	0.905	0.889	0.872	0.852	0.831	0.805
9	1.000	0.998	0.994	0.989	0.981	0.971	0.958	0.945	0.931	0.916	0.901	0.884	0.863	0.841	0.817	0.790

TABLE IV. RGD and $\overline{RGD}$ values for the GE SenoClaire tomosynthesis system.

Thickness (cm)	Angle (deg) 0	3.125	6.25	9.375	12.5	$\overline{RGD}$
2	1.000	0.999	0.996	0.990	0.982	0.994
3	1.000	1.000	0.994	0.988	0.979	0.992
4	1.000	0.999	0.993	0.986	0.974	0.990
5	1.000	0.999	0.992	0.983	0.970	0.989
6	1.000	0.999	0.993	0.983	0.969	0.989
7	1.000	0.997	0.991	0.980	0.966	0.987
8	1.000	0.998	0.991	0.979	0.963	0.986
9	1.000	0.998	0.991	0.978	0.961	0.986

values for each thickness form smooth curves. The D_gN_{TOMO} value (Eq. (3)) can then be multiplied by the entrance skin exposure to obtain the glandular dose from one tomosynthesis acquisition, as per the usual method used for mammography dose estimation. Because this report and the Wu *et al.* mammography dose data include only the CC view, resulting in a symmetric geometry acquisition about the midline of the detector, only the results for the positive projection angles are reported here.

4.C. Specific commercial and prototype breast tomosynthesis systems

Tables IV–VII provide the individual RGD and $\overline{RGD}$ values for the specific breast tomosynthesis systems included in this report, except for the Philips MicroDose system. Although $\overline{RGD}$ is sufficient to determine D_gN_{TOMO} for a tomosynthesis examination, the individual RGD values are needed if more advanced tomosynthesis acquisitions are used, such as protocols with varying tube current-exposure time product per projection angle. It should be noted that the RGD provided is not just the mean of the RGD values listed in the tables, but the mean for the complete acquisition set, so the non-zero projections are included twice in the calculation of $\overline{RGD}$, assuming a symmetric acquisition sweep.

Figure 5 shows a graph of the RGD values for the four commercial systems and the generic system for a 5 cm thick breast. It can be seen that all systems display similar trends in RGD with projection angle.

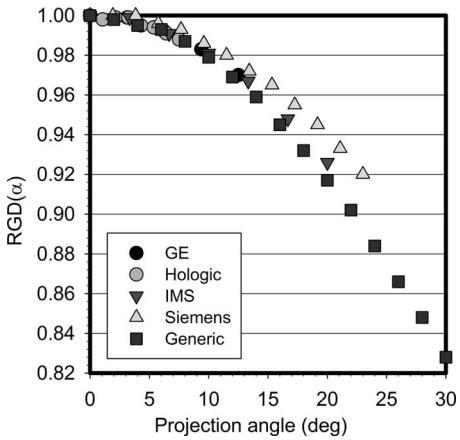

FIG. 5. RGD(α) values vs projection angle for a 5 cm thick compressed breast for the four commercial full field tomosynthesis systems and the generic system description included in this report.

Table VIII provides the D_gN_{TOMO} values for the Philips MicroDose tomosynthesis prototype system to be used with the measured "reference" air kerma values to obtain the estimate of the glandular dose, using Eq. (6).

5. DISCUSSION

This report provides the methodology and data necessary to estimate breast glandular dose for breast tomosynthesis imaging as an addition to the established mammography methodology. We have replicated the imaging model devel-

TABLE V. RGD and $\overline{RGD}$ values for the Hologic Selenia Dimensions tomosynthesis system.

Thickness (cm)	Angle (deg) 0.00	1.07	2.14	3.21	4.29	5.36	6.43	7.50	$\overline{RGD}$
2	1.000	1.000	0.998	0.997	0.997	0.996	0.996	0.994	0.997
3	1.000	0.999	1.000	0.999	0.999	0.997	0.994	0.993	0.998
4	1.000	1.000	1.000	1.000	0.998	0.997	0.995	0.991	0.998
5	1.000	0.998	0.999	0.999	0.995	0.994	0.991	0.988	0.996
6	1.000	0.999	1.000	0.997	0.996	0.994	0.992	0.988	0.996
7	1.000	1.000	0.998	0.998	0.996	0.994	0.990	0.987	0.995
8	1.000	1.000	1.000	0.998	0.997	0.995	0.990	0.987	0.996
9	1.000	1.000	1.000	0.997	0.995	0.993	0.989	0.985	0.995

TABLE VI. RGD and RGD values for the IMS Giotto TOMO tomosynthesis system.

Thickness	Angle (deg)							
(cm)	0.000	3.333	6.667	10.000	13.333	16.667	20.000	$\overline{RGD}$
2	1.000	0.998	0.996	0.988	0.980	0.969	0.955	0.984
3	1.000	0.999	0.994	0.987	0.975	0.960	0.943	0.980
4	1.000	0.998	0.993	0.983	0.971	0.954	0.935	0.976
5	1.000	0.999	0.991	0.981	0.967	0.948	0.926	0.973
6	1.000	0.998	0.989	0.980	0.963	0.942	0.920	0.970
7	1.000	0.998	0.990	0.978	0.961	0.940	0.918	0.969
8	1.000	0.998	0.990	0.976	0.958	0.937	0.915	0.968
9	1.000	0.996	0.988	0.974	0.954	0.934	0.911	0.965

oped by Wu *et al.* to minimize the differences when estimating mean glandular dose from tomosynthesis compared to that from mammography.

For consistency, the single breast size specified by Wu *et al.* was considered in this report. RGD values for other breast sizes can be calculated from fits for both the CC and MLO views published by Sechopoulos *et al.*[9] In that work, the breast model used was different from that defined by Wu *et al.*, with the main differences being: (i) inclusion of the compression paddle and breast support and cover plates in the simulations, resulting in the inclusion of their contribution to scatter dose, (ii) inclusion of the heel effect, (iii) the breast modeled with curved edges, and (iv) inclusion of air. However, a comparison of the RGD values provided in this report with those reported by Sechopoulos *et al.*[9] for the CC view, showed that the average difference in corresponding RGD is 1.2%, with a range of −6.4% to +0.3%. Therefore, as stated above, the fit equations for RGD provided by that work can be used if other breast sizes or other characteristics are needed.

As can be seen from the tables of dosimetry data for the specific breast tomosynthesis systems included in this report, the values of $\overline{RGD}$ do not deviate substantially from unity. Therefore, if the dose estimation required is for that of a "standard" tomosynthesis acquisition, i.e., constant tube current-exposure time product for all projections and symmetric acquisition angles about 0°, then, to within a 5% error, the value of $\overline{RGD}$ can be assumed to be unity and the normalized glandular dose values for mammography can be used to estimate the glandular dose for a tomosynthesis acquisition. If a more accurate estimation is needed, or if the acquisition protocol incorporates either varying tube current-exposure time products for different projection angles and/or non-symmetric projection angles about 0°, then the values provided in these tables for RGD(α) and $\overline{RGD}$ should be used.

As can be seen from Fig. 5, the RGD(α) for the different systems show the same trends in terms of variation with projection angle. Some difference can be seen, most probably introduced by the difference in position of the center of rotation among the systems, which causes a different variation in the source-to-entrance surface distance with projection angle.

The presented dosimetry model has some limitations. In the first place, and most importantly, this model does not estimate patient-specific dose values. Several enhancements would need to be made for patient-specific estimates, chief among them the use of the actual distribution of glandular tissue within the breast, as opposed to the homogeneous tissue mixture, which has been shown to introduce large uncertainties.[8,19] However, this would make the use of precalculated tabular values impossible, since there are infinite possibilities of glandular tissue distribution. Other enhancements to the model would involve the use of a more realistic breast shape, the inclusion of the mediolateral oblique (MLO) view, and the use of a more realistic x-ray field distribution, including the heel effect. However, for consistency with the existing mammography model, the assumptions and simplifications used by Wu *et al.* were maintained.

TABLE VII. RGD and $\overline{RGD}$ values for the Siemens MAMMOMAT Inspiration tomosynthesis system.

Thickness	Angle (deg)												
(cm)	0.000	1.917	3.833	5.750	7.667	9.584	11.500	13.417	15.334	17.250	19.167	21.084	23.000	$\overline{RGD}$
2	1.000	1.000	1.000	0.997	0.996	0.992	0.988	0.986	0.980	0.976	0.970	0.963	0.956	0.985
3	1.000	1.000	1.000	0.998	0.996	0.993	0.986	0.983	0.976	0.969	0.961	0.950	0.940	0.981
4	1.000	1.000	0.999	0.997	0.994	0.988	0.984	0.977	0.970	0.960	0.951	0.941	0.930	0.976
5	1.000	1.000	1.000	0.996	0.993	0.986	0.980	0.972	0.965	0.955	0.945	0.933	0.920	0.973
6	1.000	1.000	0.997	0.994	0.990	0.984	0.978	0.969	0.960	0.950	0.939	0.927	0.914	0.969
7	1.000	0.998	0.995	0.993	0.989	0.983	0.974	0.966	0.956	0.945	0.934	0.922	0.909	0.966
8	1.000	0.998	0.997	0.993	0.988	0.981	0.973	0.963	0.955	0.942	0.931	0.918	0.907	0.965
9	1.000	1.000	0.998	0.994	0.989	0.981	0.974	0.964	0.951	0.941	0.929	0.917	0.905	0.965

TABLE VIII. D_gN_{TOMO} values (mGy/mGy air kerma) for the Philips MicroDose tomosynthesis system for varying compressed breast thickness (2–9 cm), tube voltage (26–38 kVp) and glandular fraction (1%–100%).

	Glandular fraction (%)				
2 cm thick	1	25	50	75	100
26 kVp	0.527	0.501	0.475	0.448	0.424
29 kVp	0.533	0.510	0.483	0.456	0.439
32 kVp	0.582	0.551	0.531	0.505	0.481
35 kVp	0.619	0.597	0.569	0.545	0.523
38 kVp	0.645	0.627	0.602	0.574	0.556
3 cm thick					
26 kVp	0.427	0.395	0.363	0.337	0.310
29 kVp	0.440	0.409	0.382	0.353	0.329
32 kVp	0.489	0.457	0.427	0.399	0.371
35 kVp	0.528	0.494	0.464	0.438	0.410
38 kVp	0.563	0.531	0.502	0.474	0.446
4 cm thick					
26 kVp	0.355	0.321	0.290	0.265	0.243
29 kVp	0.371	0.339	0.309	0.284	0.259
32 kVp	0.419	0.384	0.352	0.326	0.301
35 kVp	0.458	0.423	0.393	0.365	0.337
38 kVp	0.494	0.458	0.428	0.399	0.371
5 cm thick					
26 kVp	0.301	0.271	0.242	0.217	0.197
29 kVp	0.320	0.290	0.260	0.236	0.213
32 kVp	0.358	0.329	0.297	0.270	0.247
35 kVp	0.398	0.366	0.334	0.306	0.282
38 kVp	0.432	0.399	0.368	0.339	0.313
6 cm thick					
26 kVp	0.259	0.229	0.203	0.181	0.163
29 kVp	0.276	0.247	0.221	0.199	0.179
32 kVp	0.319	0.287	0.260	0.234	0.212
35 kVp	0.356	0.323	0.294	0.268	0.244
38 kVp	0.388	0.350	0.323	0.295	0.272
7 cm thick					
26 kVp	0.225	0.197	0.175	0.156	0.138
29 kVp	0.244	0.215	0.193	0.172	0.155
32 kVp	0.279	0.250	0.224	0.200	0.183
35 kVp	0.317	0.286	0.260	0.233	0.214
38 kVp	0.345	0.314	0.283	0.259	0.236
8 cm thick					
26 kVp	0.200	0.174	0.153	0.137	0.121
29 kVp	0.215	0.193	0.169	0.151	0.136
32 kVp	0.252	0.225	0.200	0.181	0.163
35 kVp	0.286	0.257	0.231	0.208	0.190
38 kVp	0.312	0.284	0.256	0.233	0.212
9 cm thick					
26 kVp	0.178	0.156	0.137	0.121	0.108
29 kVp	0.194	0.171	0.151	0.135	0.121
32 kVp	0.228	0.203	0.181	0.161	0.144
35 kVp	0.260	0.233	0.209	0.188	0.170
38 kVp	0.285	0.257	0.233	0.210	0.191

ACKNOWLEDGMENTS

The authors want to thank David Dance for fruitful discussions.

APPENDIX: DOSIMETRIC DATA FOR ALTERNATIVE ACQUISITION MODE OF THE HOLOGIC SELENIA DIMENSIONS

See Table IX in the Appendix.

TABLE IX. RGD and $\overline{\text{RGD}}$ values for the Hologic Selenia Dimensions tomosynthesis system when used in the wide angular range mode (±15°).

	Angle (deg)															
Thickness (cm)	0.00	1.07	2.14	3.21	4.29	5.36	6.43	7.50	8.57	9.64	10.71	11.79	12.86	13.93	15.00	$\overline{\text{RGD}}$
2	1.000	1.001	1.000	0.998	0.997	0.997	0.996	0.993	0.992	0.990	0.987	0.983	0.980	0.978	0.975	0.991
3	1.000	1.002	0.999	1.000	0.998	0.997	0.995	0.992	0.991	0.988	0.984	0.981	0.978	0.971	0.967	0.989
4	1.000	0.998	0.999	0.997	0.996	0.994	0.992	0.989	0.987	0.984	0.981	0.976	0.971	0.967	0.962	0.986
5	1.000	1.000	0.999	0.996	0.996	0.994	0.991	0.989	0.985	0.982	0.978	0.973	0.969	0.962	0.957	0.985
6	1.000	0.999	0.998	0.997	0.996	0.993	0.991	0.988	0.984	0.979	0.975	0.971	0.965	0.960	0.953	0.983
7	1.000	1.000	1.000	0.998	0.996	0.994	0.991	0.987	0.984	0.979	0.974	0.969	0.964	0.957	0.951	0.983
8	1.000	1.001	0.998	0.998	0.996	0.993	0.991	0.986	0.982	0.977	0.972	0.966	0.960	0.954	0.948	0.981
9	1.000	1.000	0.999	0.997	0.996	0.993	0.989	0.984	0.979	0.975	0.969	0.965	0.958	0.951	0.945	0.980

[a]Author to whom correspondence should be addressed. Electronic mail: isechop@emory.edu

[1]G. R. Hammerstein, D. W. Miller, D. R. White, M. E. Masterson, H. Q. Woodard, and J. S. Laughlin, "Absorbed radiation dose in mammography," Radiology **130**, 485–491 (1979).

[2]D. R. Dance, "The Monte Carlo calculation of integral radiation dose in xeromammography," Phys. Med. Biol. **25**, 25–37 (1980).

[3]D. R. Dance, "Monte Carlo calculation of conversion factors for the estimation of mean glandular breast dose," Phys. Med. Biol. **35**, 1211–1219 (1990).

[4]X. Wu, G. T. Barnes, and D. M. Tucker, "Spectral dependence of glandular tissue dose in screen-film mammography," Radiology **179**, 143–148 (1991).

[5]X. Wu, E. L. Gingold, G. T. Barnes, and D. M. Tucker, "Normalized average glandular dose in molybdenum target-rhodium filter and rhodium target-rhodium filter mammography," Radiology **193**, 83–89 (1994).

[6]J. M. Boone, "Glandular breast dose for monoenergetic and high-energy X-ray beams: Monte Carlo assessment," Radiology **213**, 23–37 (1999).

[7]J. M. Boone, "Normalized glandular dose (DgN) coefficients for arbitrary X-ray spectra in mammography: Computer-fit values of Monte Carlo derived data," Med. Phys. **29**, 869–875 (2002).

[8]I. Sechopoulos, K. Bliznakova, X. Qin, B. Fei, and S. S. J. Feng, "Characterization of the homogeneous tissue mixture approximation in breast imaging dosimetry," Med. Phys. **39**, 5050–5059 (2012).

[9]I. Sechopoulos, S. Suryanarayanan, S. Vedantham, C. D'Orsi, and A. Karellas, "Computation of the glandular radiation dose in digital tomosynthesis of the breast," Med. Phys. **34**, 221–232 (2007).

[10]I. Sechopoulos and C. J. D'Orsi, "Glandular radiation dose in tomosynthesis of the breast using tungsten targets," J. Appl. Clin. Med. Phys. **9**, 161–171 (2008).

[11]A. K. W. Ma, D. G. Darambara, A. Stewart, S. Gunn, and E. Bullard, "Mean glandular dose estimation using MCNPX for a digital breast tomosynthesis system with tungsten/aluminum and tungsten/aluminum + silver x-ray anode-filter combinations," Med. Phys. **35**, 5278–5289 (2008).

[12]D. R. Dance, K. C. Young, and R. E. van Engen, "Estimation of mean glandular dose for breast tomosynthesis: Factors for use with the UK, European and IAEA breast dosimetry protocols," Phys. Med. Biol. **56**, 453–471 (2011).

[13]I. Sechopoulos, "A review of breast tomosynthesis. Part I. The image acquisition process," Med. Phys. **40**, 014301 (12pp.) (2013).

[14]W. T. Sobol and X. Wu, "Parametrization of mammography normalized average glandular dose tables," Med. Phys. **24**, 547–554 (1997).

[15]D. R. Dance, C. L. Skinner, K. C. Young, J. R. Beckett, and C. J. Kotre, "Additional factors for the estimation of mean glandular breast dose using the UK mammography dosimetry protocol," Phys. Med. Biol. **45**, 3225–3240 (2000).

[16]J. M. Boone, T. R. Fewell, and R. J. Jennings, "Molybdenum, rhodium, and tungsten anode spectral models using interpolating polynomials with application to mammography," Med. Phys. **24**, 1863–1874 (1997).

[17]S. Agostinelli *et al.*, "Geant4 - A simulation toolkit," Nucl. Instrum. Methods Phys. Res., Sect. A **506**, 250–303 (2003).

[18]J. Allison *et al.*, "Geant4 developments and applications," IEEE Trans. Nucl. Sci. **53**, 270–278 (2006).

[19]D. R. Dance, R. A. Hunt, P. R. Bakic, A. D. A. Maidment, M. Sandborg, G. Ullman, and G. Alm Carlsson, "Breast dosimetry using high-resolution voxel phantoms," Radiat. Prot. Dosimetry **114**, 359–363 (2005).